Articles

Novel sst$_4$-Selective Somatostatin (SRIF) Agonists. 1. Lead Identification Using a Betide Scan

Jean Rivier,*,[†] Judit Erchegyi,[†] Carl Hoeger,[‡] Charleen Miller,[†] William Low,[†] Sandra Wenger,[§] Beatrice Waser,[§] Jean-Claude Schaer,[§] and Jean Claude Reubi[§]

The Clayton Foundation Laboratories for Peptide Biology, The Salk Institute for Biological Studies, 10010 North Torrey Pines Road, La Jolla, California 92037, Department of Chemistry & Biochemistry, 0303, University of California, San Diego, 9500 Gilman Drive, La Jolla, California 92093-0303, and Division of Cell Biology and Experimental Cancer Research, Institute of Pathology, University of Berne, CH-3012 Berne, Switzerland

Hypothesizing that structural constraints in somatostatin (SRIF) analogues may result in receptor selectivity, and aiming to characterize the bioactive conformation of somatostatin at each of its five receptors, we carried out an N$^\beta$-methylated aminoglycine (Agl) scan of the octapeptide H-c[Cys^3-Phe^6-Phe^7-DTrp^8-Lys^9-Thr^{10}-Phe^{11}-Cys^{14}]-OH (SRIF numbering) (ODT-8) that is potent at all SRIF receptor subtypes (sst's) but sst$_1$. We found that H-c[Cys-LAgl-(N$^\beta$Me,benzoyl)-Phe-DTrp-Lys-Thr-Phe-Cys]-OH (**4**), H-c[Cys-Phe-LAgl(N$^\beta$Me,benzoyl)-Trp-Lys-Thr-Phe-Cys]-OH (**6**), H-c[Cys-Phe-LAgl(N$^\beta$Me,benzoyl)-DTrp-Lys-Thr-Phe-Cys]-OH (**8**), and H-c[DCys-Phe-LAgl(N$^\beta$Me,benzoyl)-DTrp-Lys-Thr-Phe-Cys]-OH (**10**) had high affinity (IC$_{50}$ = 14.3, 5.4, 5.2, and 3.4 nM, respectively) and selectivity for sst$_4$ (>50-fold over the other receptors). The L-configuration at positions 7 and 8 (L^7, L^8) yields greater sst$_4$ selectivity than the L^7, D^8 configuration (**6** versus **8**). Peptides with the D^7, L^8 (**7**) and D^7, D^8 (**9**) configurations are significantly less potent at all receptors. H-c[Cys-Phe-Phe-DTrp-LAgl(βAla)-Thr-Phe-Cys]-OH (**16**), H-c[Cys-Phe-Phe-DTrp-DAgl(βAla)-Thr-Phe-Cys]-OH (**17**), and their N$^\beta$Me derivatives at position 9 (**18**, **19**) were essentially inactive. Potent but less sst$_4$-selective were members of the Agl-scan at positions 10, H-c[Cys-Phe-Phe-DTrp-Lys-LAgl(N$^\beta$Me,HO−Ac)-Phe-Cys]-OH (**20**, IC$_{50}$ = 6.5 nM), and 11, H-c[Cys-Phe-Phe-DTrp-Lys-Thr-LAgl(N$^\beta$Me,benzoyl)-Cys]-OH (**22**, IC$_{50}$ = 6.9 nM), while the D-configuration at positions 10 (**21**) and 11 (**23**) led to reduced affinity. One of our best analogues, **8**, is an agonist when tested for its ability to inhibit forskolin-stimulated cAMP accumulation in sst$_4$-transfected CCL39 cells (EC$_{50}$ = 1.01 nM). All Agl-containing analogues were first synthesized using unresolved Fmoc-Agl(N$^\beta$Me,Boc)-OH, and the diastereomers were separated using HPLC. Chiral assignment at the Agl-containing residue was subsequently done using enzymatic degradation and by de novo synthesis in the cases of H-c[Cys-Phe-DAgl(N$^\beta$Me,benzoyl)-DTrp-Lys-Thr-Phe-Cys]-OH (**9**) and H-c[DCys-Phe-DAgl-(N$^\beta$Me,benzoyl)-DTrp-Lys-Thr-Phe-Cys]-OH (**11**), starting with the papain-resolved Fmoc-DAgl-(Boc). These results suggested that the orientation of side chains at position 6, 7, or 11 with respect to the side chains of residues 8 and 9 may be independently responsible for sst$_4$ selectivity.

Introduction

A general aim of our laboratories has been to study the tissue distribution, mechanism of action, and physiological role as well as pharmacological effects of the hypothalamic releasing hormones [thyrotropin releasing hormone (TRH),[1] gonadotropin releasing hormone (GnRH),[2,3] somatostatin (somatotropin release inhibiting factor, SRIF),[4] corticotropin releasing factor (CRF),[5] and growth hormone releasing hormone (GRF)[6,7]] in the endocrine, exocrine, and nervous systems. To achieve these goals, we need to design peptide analogues that

are (1) potent (IC$_{50}$ smaller than the corresponding IC$_{50}$ for the native ligand) and highly receptor-selective (>100-fold) peptide ligands, (2) potent and highly receptor-selective radiolabeled peptide tracers for binding assays and scintigraphy studies, (3) potent and highly receptor-selective peptide agonists, and (4) antagonists for in vitro (mechanistic) and in vivo (functional/physiological) studies. It would also be advantageous for these analogues to be resistant to degradation in biological fluids. Because some of these analogues have highly constrained structures, they are valuable tools for structural studies using NMR, as was the case for mono- and dicyclic GnRH antagonists, leading to the determination of a consensus bioactive conformation.[8]

In the case of SRIF and SRIF-28 (see Figure 1) that are short acting,[9] with five membrane-associated G

* To whom correspondence should be addressed. Phone: (858) 453-4100. Fax: (858) 552-1546. E-mail: jrivier@salk.edu.
† The Salk Institute for Biological Studies.
‡ University of California, San Diego.
§ University of Berne.

SRIF:
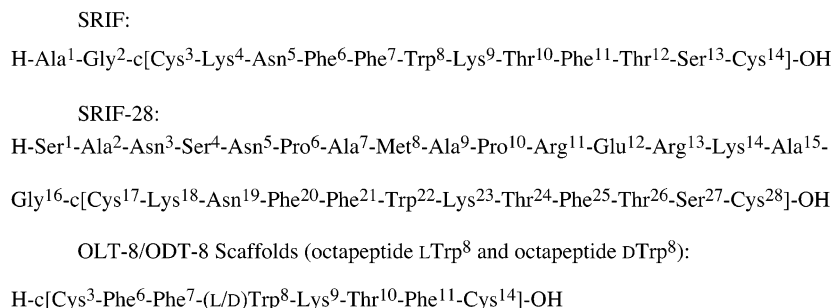
H-Ala[1]-Gly[2]-c[Cys[3]-Lys[4]-Asn[5]-Phe[6]-Phe[7]-Trp[8]-Lys[9]-Thr[10]-Phe[11]-Thr[12]-Ser[13]-Cys[14]]-OH

SRIF-28:

H-Ser[1]-Ala[2]-Asn[3]-Ser[4]-Asn[5]-Pro[6]-Ala[7]-Met[8]-Ala[9]-Pro[10]-Arg[11]-Glu[12]-Arg[13]-Lys[14]-Ala[15]-

Gly[16]-c[Cys[17]-Lys[18]-Asn[19]-Phe[20]-Phe[21]-Trp[22]-Lys[23]-Thr[24]-Phe[25]-Thr[26]-Ser[27]-Cys[28]]-OH

OLT-8/ODT-8 Scaffolds (octapeptide LTrp[8] and octapeptide DTrp[8]):

H-c[Cys[3]-Phe[6]-Phe[7]-(L/D)Trp[8]-Lys[9]-Thr[10]-Phe[11]-Cys[14]]-OH

Figure 1. Primary structures of SRIF, SRIF-28, and OLT-8/ODT-8 scaffolds, including residue numbering of SRIF as used throughout parts 1–4.

R_1 = H or CH_3
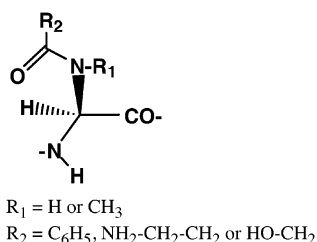R_2 = C_6H_5, NH_2-CH_2-CH_2 or HO-CH_2

Figure 2. General structure of betidamino acids derived from the aminoglycine (Agl) scaffold.

protein-coupled receptor subtypes (sst's),[10–17] fulfilling these goals is daunting. SRIF is a major endocrine hormone with multiple physiological actions[18–28] modulated by one or more of these receptors. The biological role, as well as the cellular distribution of each receptor subtype, is far from being completely understood. Availability of receptor subtype-selective ligands is critical to our understanding of SRIF's physiological role and pharmacological potential. Indeed, we have recently described sst$_1$-selective analogues that fulfill criteria 1–3,[29] and analogues that bind to sst$_3$ that fulfill criteria 1, 2, and 4.[30] We concluded from these studies that each SRIF receptor recognized a unique conformation of SRIF and that receptor selectivity could be achieved by limiting the number of three-dimensional structures it can assume to match the requirements of a given receptor. In other words, the bioactive conformations of the receptor-selective SRIF analogues had to be different from each other, yet they would be available to SRIF.

There are several approaches to restrain the structure of peptides: N^α- and C^α-methylation as well as cyclization, for example, will constrain backbone conformations. Additionally, β-methylation will restrict side-chain conformations. However, because the chiral synthesis or resolution and characterization of the four stereoisomers is arduous, we recently proposed an alternative approach. In four consecutive papers we are describing a general strategy based on the use of betidamino acids (betidamino acid scan of ODT-8, part 1) for lead discovery and β-methyl amino acids (part 2)[31] for further enhancement of affinity and selectivity of sst$_4$-selective ligands that fulfill criteria 1–3 (part 3).[32] Part 4 describes NMR studies that identified structural features that may be responsible for sst$_4$ selectivity.[33] Betidamino acids are monoacylated derivatives of α-aminoglycine, as shown in Figure 2. The synthesis of N^α-Boc,N^β-Fmoc-aminoglycine was originally described by Qasmi et al.[34] More recently, we published the optical resolution of this derivative[35] as well as the synthesis

of methylated derivatives.[36] We had demonstrated that betidamino acids were compatible with biological activity in more than one system (GnRH,[37] CRF[38]). Additionally, we have validated our strategy with the discovery that H$_2$N-CO-c[DCys[3]-Phe[6]-Tyr[7]-DAgl[8](N^βMe,2naphthoyl)-Lys[9]-Thr[10]-Phe[11]-Cys[14]]-OH (des-AA[1,2,4,5,12,13]-[DCys[3],-Tyr[7],DAgl[8](N^βMe,2naphthoyl)]Cbm-SRIF) is a potent and highly sst$_3$-selective antagonist.[30] In short, while the N^β-monoacylated betidamino acids are homologous to standard amino acids, the N^β-monoacylated and N^β-methylated betidamino acids are homologous to the β-methylated amino acids without a side-chain asymmetric center. Because N^β-methylated betidamino acids are easy to obtain as compared to the corresponding β-methyl amino acids, we hypothesized that the former could be used to scan bioactive structures to identify those residues most likely to benefit from β-methylation. We report here the N^β-methylated aminoglycine scan of H-c[Cys-Phe-Phe-DTrp-Lys-Thr-Phe-Cys]-OH (ODT-8) and partial scan of H-c[Cys-Phe-Phe-Trp-Lys-Thr-Phe-Cys]-OH (OLT-8) (see Figure 1 for residue numbering) that led to the identification of sst$_4$-selective agonists and the definition of general principles for the development of even more potent and selective analogues of somatostatin.

Results and Discussion

We have used unresolved N^α-Boc,N^β-Fmoc-aminoglycine,[34,39] and N^α-Boc,N^β-(CH$_3$)Fmoc-aminoglycine[36,39] as templates for the introduction of betidamino acids in ODT-8 (**3**) and OLT-8 (**2**). These were the first members of the short/mini somatostatins with significant potency when tested for their ability to inhibit growth hormone release from rat pituitary cells in culture and to inhibit glucagon and insulin in the rat.[40,41] Their binding affinity for human sst's is shown in Table 1.

All the analogues shown in Table 1 were synthesized either manually or automatically on a chloromethylated resin using the Boc strategy. The peptides were purified using preparative RP-HPLC in at least two different solvent systems (TEAP pH 2.25 and 0.1% TFA on C$_{18}$ silica) and characterized as shown in Table 1 using RP-HPLC, CZE, and mass spectrometry as published earlier.[29] Because the starting Boc-Agl(Fmoc)-OH initially used in the scans was not resolved, we made the diastereomeric mixtures that were then separated by HPLC and fully characterized. The enzymatic cleavage patterns of all diastereomers were compared to show that the L-aminoglycine-containing analogue was hydrolyzed when the D-amino acid-containing analogue was not. In two cases (**9** and **11**), the stereochemistry

Table 1. Physicochemical Properties and sst_{1-5} Binding Affinities (IC_{50}, nM) of sst_4-Selective Analogues and Control Peptides

no.	compd	purity (%) HPLC[a]	CZE[b]	MS[c] M(mono) calcd	MH⁺(mono) obsd	IC_{50} (nM)[d] sst_1	sst_2	sst_3	sst_4	sst_5
1	somatostatin-28	98	98	3146.5	3147.7	3.9 ± 0.3	3.3 ± 0.2	7.1 ± 0.7	3.8 ± 0.3	3.9 ± 0.3
2	H-c[Cys-Phe-Phe-Trp-Lys-Thr-Phe-Cys]-OH (OLT-8)	97	98	1078.44	1079.4	5.3 ± 0.7 (3)	130 ± 65 (3)	13 ± 0.7 (3)	0.7 ± 0.3 (3)	14 ± 4 (3)
3	H-c[Cys-Phe-Phe-DTrp-Lys-Thr-Phe-Cys]-OH (ODT-8)	>94	98	1078.44	1079.2	27 ± 3 (4)	41 ± 9 (6)	13 ± 3 (4)	1.8 ± 0.7 (4)	46 ± 27 (3)
4	H-c[Cys-LAgl(NβMe,benzoyl)-Phe-DTrp-Lys-Thr-Phe-Cys]-OH	92	98	1121.45	1122.5	667 ± 164 (3)	374 ± 87 (4)	>10K (3)	14 ± 6 (3)	>1000 (3)
5	H-c[Cys-DAgl(NβMe,benzoyl)-Phe-DTrp-Lys-Thr-Phe-Cys]-OH	97	97	1121.45	1122.4	>10K (2)	>1000 (3)	>10K (2)	>1000 (2)	>1000 (2)
6	H-c[Cys-Phe-LAgl(NβMe,benzoyl)-Trp-Lys-Thr-Phe-Cys]-OH	99	99	1121.45	1122.3	>10K (2)	>1000 (2)	403 (500; 305)	5.4 (2.8; 7.9)	>1000 (2)
7	H-c[Cys-Phe-DAgl(NβMe,benzoyl)-Trp-Lys-Thr-Phe-Cys]-OH	95	97	1121.45	1122.4	>10K (2)	>1000 (2)	725 (650; 799)	133 (90; 176)	>1000 (2)
8	H-c[Cys-Phe-LAgl(NβMe,benzoyl)-DTrp-Lys-Thr-Phe-Cys]-OH	93	87	1121.45	1122.5	>1000 (3)	460 ± 87 (4)	447 ± 169 (3)	5.2 ± 1.1 (3)	768 ± 129 (3)
9	H-c[Cys-Phe-DAgl(NβMe,benzoyl)-DTrp-Lys-Thr-Phe-Cys]-OH	97	98	1121.45	1122.5	>10K (2)	>1000 (3)	>1000 (2)	153 (88; 217)	>1000 (2)
10	H-c[DCys-Phe-LAgl(NβMe,benzoyl)-DTrp-Lys-Thr-Phe-Cys]-OH	98	94	1121.45	1122.6	>1000 (2)	533 (390; 676)	382 (260; 504)	3.4 (5.1; 1.7)	460 (260; 659)
11	H-c[DCys-Phe-DAgl(NβMe,benzoyl)-DTrp-Lys-Thr-Phe-Cys]-OH	96	95	1121.45	1122.4	>1000 (2)	>1000 (2)	136 (90; 181)	31 (35; 27)	>1000 (2)
12	H-Tyr-c[Cys-Phe-LAgl(NβMe,benzyl)-Trp-Lys-Thr-Phe-Cys]-OH	99	98	1284.51	1285.3	>1000 (2)	>10K (2)	319 (150; 487)	24 (18; 29)	>1000 (2)
13	H-Tyr-c[Cys-Phe-DAgl(NβMe,benzoyl)-Trp-Lys-Thr-Phe-Cys]-OH	86	88	1284.51	1285.3	>1000 (2)	>1000 (2)	453 (500; 405)	159 (140; 178)	>1000 (2)
14	H-Tyr-c[Cys-Phe-LAgl(NβMe,benzoyl)-DTrp-Lys-Thr-Phe-Cys]-OH	99	97	1284.51	1285.4	>10K (3)	594 ± 79 (3)	273 ± 74 (3)	18 ± 3 (3)	34 ± 15 (3)
15	H-Tyr-c[Cys-Phe-DAgl(NβMe,benzoyl)-DTrp-Lys-Thr-Phe-Cys]-OH	99	99	1284.51	1285.4	>10K (2)	>1000 (2)	>1000 (2)	56 (22; 90)	>1000 (2)
16	H-c[Cys-Phe-Phe-DTrp-LAgl(βAla)-Thr-Phe-Cys]-OH	99	92	1093.42	1094.6	>10K	>1000 (2)	>1000	>10K	>10K
17	H-c[Cys-Phe-Phe-DTrp-DAgl(βAla)-Thr-Phe-Cys]-OH	98	99	1093.42	1094.6	>10K	>1000 (2)	>1000	>1000	>10K
18	H-c[Cys-Phe-Phe-DTrp-LAgl(NβMe,βAla)-Thr-Phe-Cys]-OH	95	97	1107.43	1108.5	>1000	>1000	>1000	>1000	>1000
19	H-c[Cys-Phe-Phe-DTrp-DAgl(NβMe,βAla)-Thr-Phe-Cys]-OH	97	97	1107.43	1108.4	>10K (2)	>10K (3)	>1000 (2)	429 (378; 480)	>1000 (2)
20	H-c[Cys-Phe-Phe-DTrp-Lys-LAgl(NβMe,HO−Ac)-Phe-Cys]-OH	95	96	1121.45	1122.5	45 ± 8.73 (4)	>1000 (4)	>1000 (3)	6.5 (5.6; 7.3)	211 ± 85 (3)
21	H-c[Cys-Phe-Phe-DTrp-Lys-DAgl(NβMe,HO−Ac)-Phe-Cys]-OH	91	94	1121.45	1122.5	860	>1000 (3)	>1000 (2)	38 (54; 21)	389 (530; 247)
22	H-c[Cys-Phe-Phe-DTrp-Lys-Thr-LAgl(NβMe,benzoyl)-Cys]-OH	78	78	1121.45	1122.4	>10K	455 (390; 520)	235 (340; 130)	6.9 (9.2; 4.5)	220 (210; 230)
23	H-c[Cys-Phe-Phe-DTrp-Lys-Thr-DAgl(NβMe,benzoyl)-Cys]-OH	86	84	1121.45	1122.4	>10K (3)	>1000 (4)	>1000 (3)	80 ± 23 (3)	>1000 (3)
24	L-803,087 (Merck)[45]					>1000 (4)	>1000 (4)	>1000 (4)	4.2 ± 1.9 (3)	>10K (4)

[a] Percent purity determined by HPLC using buffer system: A = TEAP (pH 2.5) and B = 60% CH_3CN/40% A with a gradient slope of 1% B/min, at flow rate of 0.2 mL/min on a Vydac C_{18} column (0.21 × 15 cm, 5 μm particle size, 300 Å pore size). Detection at 214 nm. [b] Capillary zone electrophoresis (CZE) was done using a Beckman P/ACE System 2050 controlled by an IBM Personal System/2 model 50Z and using a ChromJet integrator; field strength of 15 kV at 30 °C. Mobile phase: 100 mM sodium phosphate (85:15, H_2O:CH_3CN), pH 2.50, on a Supelco P175 capillary (363 μm o.d × 75 μm i.d. × 50 cm length). Detection at 214 nm. [c] The calculated *m/z* of the monoisotope compared with the observed $[M + H]^+$ monoisotopic mass. [d] The IC_{50} values (nM) were derived from competitive radioligand displacement assays, reflecting the affinities of the analogues for the cloned somatostatin receptors using the nonselective ¹²⁵I-[Leu⁸,DTrp²²,Tyr²⁵]SRIF-28 as the radioligand. Mean value ± SEM when $N ≥ 3$ (shown in parentheses). In the other cases, mean is shown with single values in parentheses.

at the Agl residue was confirmed by comparison of the HPLC retention times of each diastereomer with that of the same analogue synthesized with resolved (*R*)-Boc,Fmoc-aminoglycine.[35] In brief, **9** and **11** were synthesized with the papain-resolved, optically active (*R*)-Boc,Fmoc-aminoglycine (same as Boc-LAgl(Fmoc)-OH or Fmoc-DAgl(Boc)-OH), which was also synthesized from (*S*)-*Z*-Ser to confirm the configuration of the chiral center of aminoglycine.[35] The Nβ-methyl group was introduced on the resin by the method of Kaljuste.[30,42] In short, after coupling Fmoc-DAgl(Boc)-OH, the side-chain-protecting Boc group was removed as usual, and the resulting free amino group was reacted with 4,4′-dimethoxydityl chloride (Dod-Cl), followed by reductive methylation of the Dod-alkylated amino group, treating the resin with formaldehyde and sodium cyanoborohy-

dride in NMP. After the removal of the Dod group with TFA (60%), the free secondary amino group was acylated with benzoyl chloride. Removal of the Nα-Fmoc protecting group with 20% piperidine in NMP in two successive 5- and 15-min treatments allowed the elongation of the peptide backbone until completion of the peptide. The resulting peptides (**9** and **11**) coeluted on HPLC, with the first eluting diastereomers of the pairs (**8** + **9** and **10** + **11**) obtained with unresolved Fmoc-D/LAgl(NβMe,Boc)-OH.

The compounds were tested for their ability to bind to the five human SRIF receptor subtypes in competitive experiments using ¹²⁵I-[Leu⁸,DTrp²²,Tyr²⁵]SRIF-28 as radioligand. Cells stably expressing the cloned five human sst's were grown as described previously.[43] Cell membrane pellets were prepared and receptor autora-
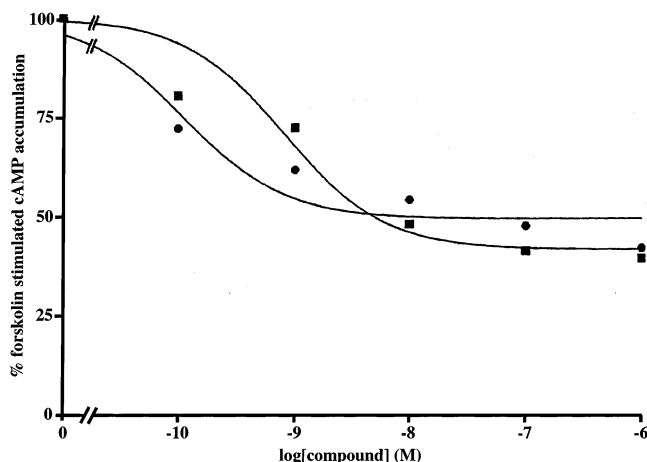
Figure 3. Effect of various concentrations of somatostatin-28 (SRIF-28), and the sst$_4$-selective agonist **8** on forskolin-stimulated cAMP accumulation in CCL39 cells expressing sst$_4$. Concentration−response curves were obtained with increasing concentrations of SRIF-28 (●) and **8** (■). Data are expressed as % forskolin-stimulated cAMP accumulation. The plot represents the mean of two independent experiments. Analogue **8** behaves as an agonist.

diography was performed as depicted in detail previously.[43] The binding affinities are expressed as IC$_{50}$ values that were calculated after quantification of the data using a computer-assisted image-processing system as described previously.[43,44] Control peptides include SRIF-28, OLT-8 (**2**), ODT-8 (**3**), and the sst$_4$-selective non-peptide L-803,087 (**24**).[45] One of the most potent analogues (**8**) was evaluated for its agonist/antagonist properties by measuring inhibition of forskolin-stimulated cyclic adenosine monophosphate (cAMP) production (Figure 3).[30]

From the affinities of OLT-8 (**2**) and ODT-8 (**3**) for the five sst's (Table 1), it is notable that both have greater affinity (5-fold and 2-fold, respectively) for sst$_4$ than SRIF-28 while having similar affinities at the other four receptors. On the basis of this observation, we concluded that the octapeptide scaffold with either the L- or DTrp at position 8 would be a good lead for the design of sst$_4$-selective analogues. The first diastereomers, **4** (IC$_{50}$ = 14.3 nM at sst$_4$) and **5** (IC$_{50}$ > 1000 nM at sst$_4$), have the Phe at position 6 substituted by the N$^\beta$-methylated betide phenylalanine. Whereas **4** gained in sst$_4$ selectivity as compared to **3**, it also lost significant affinity (10-fold), while **5** is inactive at all receptors. Substitution of Phe^7 by L-N$^\beta$Me-betidePhe^7 in **2** yielded **6** with >80-fold sst$_4$ selectivity and high sst$_4$ affinity (IC$_{50}$ = 5.4 nM). On the other hand, substitution of Phe^7 by D-N$^\beta$Me-betidePhe^7 in **2** yielded **7** with considerable loss of binding affinity at all sst's. Interestingly, the results are almost parallel when Phe^7 was substituted by L-N$^\beta$Me-betidePhe^7 and D-N$^\beta$Me-betidePhe^7 in **3** to yield **8** and **9**, respectively. sst$_4$ selectivity of **8** is again >80-fold with retention of high affinity (IC$_{50}$ = 5.2 nM), while **9** is inactive at all receptors, except maybe at sst$_4$ (IC$_{50}$ = 153 nM). Compound **8** was found to be an agonist in its ability to inhibit forskolin-induced cAMP accumulation with an EC$_{50}$ value of 1.01 nM, compared to a value of 0.37 nM for SRIF-28 (*n* = 2). Figure 3 shows that **8** behaves similarly to SRIF-28: not only does it inhibit forskolin-stimulated cAMP accumulation

to the same level as SRIF-28, but it also does it at similar concentrations.

The observation of Bass et al.,[46,47] demonstrating that inversion of chirality at position 3 of the agonist Ac-Phe^2(4NO$_2$)-c[Cys^3-Tyr^7-DTrp^8-Lys^9-Thr^{10}-Cys^{14}]-DTyr^{15}-NH$_2$ to Ac-Phe^2(4NO$_2$)-c[DCys^3-Tyr^7-DTrp^8-Lys^9-Thr^{10}-Cys^{14}]-DTyr^{15}-NH$_2$ yielded an antagonist, was followed by contributions of Hocart et al.[48,49] and Rajeswaran et al.[50] suggesting that this modification may be generally applicable for the generation of SRIF antagonists. This led us to investigate the influence of the introduction of DCys^3 in **8** and **9** to yield **10** and **11**. Again, the LAgl^7(N$^\beta$Me,benzoyl)-containing **10** is more potent and selective than the corresponding DAgl^7(N$^\beta$Me,benzoyl)-containing **11**. In fact, **10** is the most potent and sst$_4$-selective analogue in this series and is an agonist in its ability to inhibit forskolin-induced cAMP accumulation (data not shown).

To generate an iodinatable analogue, a tyrosine residue was introduced at the N-terminus of **6**−**9** to yield **12**−**15**. As shown in Table 1, these analogues lost significant affinity (IC$_{50}$ > 18 nM) for sst$_4$ and therefore some selectivity, too. At this point, we stopped following this lead to pursue it with the use of β-methyl amino acids (see part 2).[31]

Substitution of Lys^9 in **2** by N$^\beta$Me-betideLys [LAgl^9-(N$^\beta$Me,βAla)] resulted in two inactive analogues, **18** and **19**. This was not surprising in view of the recognized importance of lysine at position 9 for binding to all sst's.[51]

Scanning position 10 of **3** with N$^\beta$Me-betideThr yielded **20** and **21**. It is noteworthy that **20** retained significant affinity at both sst$_1$ (IC$_{50}$ = 45 nM) and sst$_4$ (IC$_{50}$ = 6.5 nM) while remaining inactive at all other sst's. It should be noted that the diastereomer **21** also retained some sst$_4$ (IC$_{50}$ = 38 nM) and sst$_5$ (IC$_{50}$ = 389 nM) affinity.

Finally, introduction of N$^\beta$Me-betidePhe at position 11 of **3** yielded the L-diastereomer **22**, with high affinity for sst$_4$ (IC$_{50}$ = 6.9 nM) and limited selectivity over the other receptors (ca. 20-fold).

In conclusion, scanning of ODT-8 and OLT-8 with the corresponding β-methylated betidamino acids at positions 6, 7, 9, 10, and 11 yielded several analogues with high sst$_4$ affinity and selectivity (**4**, **6**, **8**, **10**, and **22**). This family of compounds appears to represent agonists in their ability to inhibit forskolin-induced cAMP accumulation, since not only **8** but also **6** and **10** (data not shown) showed this property. Our efforts to derive useful betidamino acid-containing sst$_4$-selective radio-iodinatable ligands were, however, unsuccessful. Structure−activity relationship studies suggested interesting new substitutions that proved to be beneficial (see parts 2[31] and 3[32] of this series).

Experimental Section

Abbreviations. The abbreviations for the common amino acids are in accordance with the recommendations of the IUPAC−IUB Joint Commission on Biochemical Nomenclature (*Eur. J. Biochem.* **1984**, *138*, 9−37). The symbols represent the L-isomer except when indicated otherwise. Additional abbreviations: Agl, aminoglycine; Boc, *tert*-butoxycarbonyl; Bzl, benzyl; Z(2Br), 2-bromobenzyloxycarbonyl; Z(2Cl), 2-chlorobenzyloxycarbonyl; Cbm, carbamoyl (NH$_2$−CO−); CZE, capillary zone electrophoresis; DIC, *N,N*-diisopropylcarbodiimide; DIPEA, diisopropylethylamine; Fmoc, 9-fluorenylmethoxycarbonyl; HOBt, 1-hydroxybenzotriazole; IBMX, 3-isobutyl-I-

methylxanthine; Mob, 4 -methoxybenzyl; Nal, 3-(2-naphthyl)-alanine; NMP, *N*-methylpyrrolidinone; OBzl, benzyl ester; SRIF, somatostatin; sst's, SRIF receptors; TEA, triethylamine; TEAP, triethylammonium phosphate; TFA, trifluoroacetic acid.

Peptide Synthesis. Peptides were synthesized by the solid-phase approach either manually or on a CS-Bio peptide synthesizer, model CS536.[52] Peptide couplings were mediated for 1 h by DIC in CH_2Cl_2 or NMP and monitored by the qualitative ninhydrin test. A 3-equiv excess of amino acid based on the original substitution of the resin was used in most cases. Boc removal was achieved with trifluoroacetic acid (60% in CH_2Cl_2, 1−2% *m*-cresol) for 20 min. An isopropyl alcohol (1% *m*-cresol) wash followed TFA treatment, and then successive washes with triethylamine solution (10% in CH_2Cl_2), methanol, triethylamine solution, methanol, and CH_2Cl_2 completed the neutralization sequence. The completed peptide was then cleaved from the resin by HF containing the scavengers anisole (10% v/v) and methyl sulfide (5% v/v) for 60 min at 0 °C. The diethyl ether-precipitated crude peptides were cyclized in 75% acetic acid (200 mL) by addition of iodine (10% solution in methanol) until the appearance of a stable orange color. Forty minutes later, ascorbic acid was added to quench the excess of iodine. All Agl-containing peptides were synthesized using the unresolved Boc,Fmoc-Agl. Additionally, **9** and **11** were synthesized starting with Fmoc-DAgl(Boc)-OH (see below).[35]

Synthesis of H-c[Cys³-Phe⁶-DAgl⁷(N$^\beta$Me,benzoyl)-DTrp⁸-Lys⁹-Thr¹⁰-Phe¹¹-Cys¹⁴]-OH (SRIF numbering) (9) and H-c[DCys³-Phe⁶-DAgl⁷(N$^\beta$Me,benzoyl)-DTrp⁸-Lys⁹-Thr¹⁰-Phe¹¹-Cys¹⁴]-OH (11) with Optically Active Fmoc-DAgl-(Boc)-OH. After coupling Fmoc-DAgl(Boc)-OH in position 7, the side-chain-protecting Boc group was removed with 60% TFA, washed, and neutralized, and to the 0.9-g peptide resin (0.36 mmol/g) swollen in dichloromethane was added Dod-Cl (130 mg, 0.5 mmol) along with DIEPA (500 μL). The mixture was shaken for an hour to complete the alkylation. The resin was washed, and shaken after the addition of formaldehyde (2 mL, 37% solution) in NMP (18 mL) and acetic acid (100 μL). After 5 min, sodium cyanoborohydride (300 mg) was added, and the mixture was shaken for 60 min. After the removal of the Dod group with TFA (60%) for 30 min, benzoyl chloride (500 μL) was used to acylate the free secondary amino group of the side chain. Removal of the N$^\alpha$-Fmoc protecting group with 20% piperidine in NMP in two successive 5- and 15-min treatments was followed by the standard elongation protocol until completion of the peptide. The peptides were cleaved, deprotected, and cyclized as described above.

Purification of Peptides. The crude, lyophilized peptides were purified by preparative RP-HPLC[53] on a 5-cm × 30-cm cartridge, packed in the laboratory with reversed-phase 300 Å Vydac C₁₈ silica (15−20 μm particle size) using a Waters Associates Prep LC/System 500A system. The peptides eluted with a flow rate of 100 mL/min using a linear gradient of 1% B per 3-min increase from the baseline % B (eluent A = 0.25 N TEAP, pH 2.25; eluent B = 60% CH₃CN, 40% A). All peptides were subjected to a second purification step carried out with eluents A = 0.1% TFA in water and B = 60% CH₃-CN/40% A on the same cartridge, using a linear gradient of 1% B per min increase from the baseline % B. Analytical HPLC screening of the purification was performed on a Vydac C₁₈ column (0.46 × 25 cm, 5 μm particle size, 300 Å pore size) connected to a Rheodyne injector, two Beckman 100A pumps, a model 420 system controller programmer, a Kratos 750 UV detector, and a Houston Instruments D-5000 strip chart recorder. The fractions containing the product were pooled and subjected to lyophilization. The final yield for these purified peptides was about 5%.

Characterization of SRIF Analogues. (See Table 1 footnote.) The purity of the final peptides was determined by analytical RP-HPLC performed with a linear gradient using 0.1 M TEAP, pH 2.5, as eluent A and 60% CH₃CN/40% A as eluent B on a Hewlett-Packard Series II 1090 liquid chromatograph connected to a Vydac C₁₈ column (0.21 × 15 cm, 5 μm particle size, 300 Å pore size), controller model 362, and a

Think Jet printer. CZE analysis was performed as described earlier.[54] Peptides are >90% pure by HPLC and CZE in most cases: **13** and **23** still contained 5−10% of the earlier-eluting diastereomers **12** and **22**, respectively. Compound **22**, on the other hand, was not significantly contaminated with **23** (<3%). Mass spectra (MALDI-MS) were measured on an ABI-Perspective DE-STR instrument. The instrument employs a nitrogen laser (337 nm) at a repetition rate of 20 Hz. The applied accelerating voltage was 20 kV. Spectra were recorded in delayed extraction mode (300 ns delay). All spectra were recorded in the positive reflector mode. Spectra were sums of 100 laser shots. Matrix α-cyano-4-hydroxycinnamic acid was prepared as saturated solutions in 0.3% trifluoroacetic acid in 50% acetonitrile. The observed monoisotopic $(M + H)^+$ values of each peptide corresponded with the calculated $(M + H)^+$ values.

Determination of the Stereochemistry of Agl in the Peptides. Since the L- and D-enantiomers of Boc-Agl(Fmoc)-OH and Boc-Agl(N$^\beta$Me,Fmoc)-OH, used for the synthesis of peptides, were not resolved initially, two diastereomers were generated, isolated, and tested. Resolution of the L- from the DAgl-containing peptides was achieved using RP-HPLC.[53,55] The absolute configuration of the Agl was deduced from enzymatic hydrolysis studies with aminopeptidase M, carboxypeptidase A, trypsin, and α-chymotrypsin, respectively. Peptides **2** and **3** were used as controls to follow the specificity of all enzymes as well as the kinetics of degradation.

Aminopeptidase M is a metalloprotease, which can hydrolyze peptides at a free α-amino group of L-amino acids (except for X-Pro bonds and the amino groups of Asp, Gln, or βAla). Aminopeptidase M was employed to determine the absolute configuration of Agl in **4−9** and **12−15**. The hydrolysis of the peptides was monitored by RP-HPLC. When it was possible, the mass of the resulting fragments was determined by MALDI mass spectrometry. The observed and calculated masses for the predicted degradation products were compared. The treatment of **6** and **12** with aminopeptidase M resulted in very hydrophilic products. The nonidentifiable small mass values of these fragments (the matrix shows several denominations in this low range as well) indicated that the peptide had been completely hydrolyzed, providing evidence that these analogues contained the L-enantiomer of Agl in their sequence. The treatment of both **7** and **13** with aminopeptidase M for up to 5 weeks resulted in products with a mass of 771.31. This mass could be assigned to H-Agl(N$^\beta$Me,benzoyl)-Trp-Lys-Thr-Phe-OH. This observation showed that the hydrolysis stopped at the Agl residue; thus, analogues **7** and **13** contained the D-enantiomer of the Agl derivative. Analogues **4**, **5**, **8**, **9**, **14**, and **15** contain a D-residue at position 8 (DTrp); therefore, a complete enzymatic hydrolysis could not be expected for any of these compounds. The treatment of **5** with aminopeptidase M for 42 h did not result in any degradation product, but the same treatment of **4** resulted in the complete disappearance of the starting material and the appearance of several very hydrophilic new fragments. This suggests that **5** contained the DAgl derivative in the sequence, resulting in its resistance to the enzymatic hydrolysis. The enzymatic hydrolysis of **8**, **9** and **14**, **15** with aminopeptidase M for 5 days showed different patterns, as followed by RP-HPLC. A fragment with a mass of 771.31 from **9** and **15** (similar to what had been observed for **7** and **13**) could be identified, suggesting that **9** and **15** contained the D-enantiomer of the Agl derivative. These observations were in agreement with the finding that **9**, synthesized with papain-resolved, optically active DAgl,[35] *N*-methylated on the resin,[42] coeluted on RP-HPLC with the earlier-eluting diastereomer obtained from the synthesis with unresolved Agl derivative. Enzymatic hydrolysis of the peptides from both origins followed the same kinetics and fingerprint of degradation. Control peptide **2**, containing all L-amino acids, was completely hydrolyzed with aminopeptidase M after 3 h. The aminopeptidase M-mediated hydrolysis of **3**, containing a DTrp at position 8, for 5 weeks resulted in a product with a mass of 581.27. This mass could be assigned to that of H-Trp-

Lys-Thr-Phe-OH, showing that further hydrolysis was stopped at the DTrp residue.

Determination of the absolute configuration at the α-carbon of Agl(βAla) and Agl(N$^\beta$Me,βAla) in peptides **16**−**19** needed a different approach since these amino acids were introduced into the sequence after DTrp[8], which blocks further cleavage by aminopeptidase M, as observed in the case of **3**. These analogues were digested with carboxypeptidase A, which preferentially cleaves off L-amino acids with aromatic or branched side chains starting at the C-terminus. Digestion of disulfide-bridge-containing peptides with carboxypeptidase A can be limited, if not impossible. First, we tried to hydrolyze **2** and **3** to find out if this method could be applied. The degree of hydrolysis for peptides **2** and **3** was 35% and 92% starting material and 65% and 8% hydrolyzed products, respectively, after 7 days, suggesting that some hydrolysis could be achieved even in the DTrp-containing analogue **3**. Peptides **16**−**19** were exposed to carboxypeptidase A digestion for 7 days. Analogue **17** showed no sign of any hydrolysis as followed by HPLC, while **16** slowly degraded, with 85% of the starting material remaining intact under the same conditions, suggesting that **16** contained the LAgl derivative in its sequence. Analogue **19** was quite resistant to carboxypeptidase A's digestion, retaining 95% integrity after 7 days. Its diastereomer **18**, on the other hand, degraded 50% under the same conditions and was therefore assumed to contain the LAgl residue. Carboxypeptidase A did not hydrolyze **20**−**23** after 5 days of incubation.

Trypsin, which is highly specific toward positively charged side chains with lysine and arginine, was able to open the ring structure of **20**−**23** after the lysine residue, resulting in products that eluted earlier on the RP-HPLC and showed higher mass by 18. The rate of reactions was very much different. Because 75% of **20** could be hydrolyzed in 5 days, while **21** remained essentially intact, we suggest that **20** contains the L-isomer of the Agl derivative and **21** its enantiomer. Interestingly, a faster reaction rate could be observed in the case of **22**. Indeed, no starting material could be detected after digestion of **22** with trypsin for 1 day, while 95% of **23** remained intact under the same conditions, suggesting that **22** contained the L-isomer of the Agl derivative and **23** its enantiomer. To explain the difference in reaction rates of these enzymatic hydrolyzes, we propose that in **20**, the Agl derivative bonded to the Lys residue limits the access of trypsin to the cleavage site more than in the case of **22**, in which a threonine follows the lysine prior to the aminoglycine derivative. The enzymatic hydrolysis of our controls (**2** and **3**) with trypsin showed similar results, in that **2** fully hydrolyzed (100%) within 4 h, whereas the presence of the DTrp[8] in the sequence of **3** slowed the rate of the hydrolysis to 35%.

In **10** and **11**, the Agl derivative has an adjacent D-amino acid (DTrp) and the peptide sequence starts with a D-amino acid (DCys). In this case, we anticipated that **10** and **11** could be labile to α-chymotrypsin, since there are two Phe residues in their sequence. However, we also expected the rates of hydrolysis to be different, depending on the presence or absence of a DAgl derivative. After 1 week, **11** retained 60% integrity while a hydrolysis product, which eluted faster on RP-HPLC, showed an 18-mass-unit increase, suggesting that the ring structure had opened. Under the same conditions, only 25% of **10** remained intact, while all hydrolysis products had lower masses and eluted faster on RP-HPLC, suggesting that the peptide was further hydrolyzed to smaller fragments after ring-opening and that this analogue had to contain the LAgl derivative. The hydrolysis of **3** with α-chymotrypsin was very slow compared to that of **2**. After 2 h, no starting material could be detected in the hydrolysis products of **2**, while only 2% of **3** had been hydrolyzed. The presence of two D-amino acids in **10** and three D-amino acids in **11** explains the difference in the rate of hydrolysis with this enzyme.

All enzymatic hydrolyses were carried out according to the protocols suggested by the manufacturers. Briefly, aminopeptidase M (Roche, 25 μL = 0.5 unit) was added to peptide (0.1 μmol) dissolved in 100 μL of 0.06 M sodium phosphate buffer (pH = 7.0), and the hydrolysis was followed by RP-HPLC for

one month. Carboxypepdiase A (Sigma, 5 μL = 5 units) with 10% LiCl (50 μL) was added to peptide (0.1 μmol) dissolved in 0.025 M Tris buffer (100 μL, pH = 7.6) containing 0.1 M NaCl, and the hydrolysis was followed by RP-HPLC for one week. α-Chymotrypsin (Sigma, 0.5 μg) in 0.01 N HCl (50 μL) was added to peptide (0.025 μmol) dissolved in 0.08 M Tris buffer (pH = 7.8, 50 μL), and the hydrolysis was followed by RP-HPLC for one week. Trypsin (Roche, 5 μg) in 0.05% TFA (20 μL) was added to peptide (0.02 μmol) dissolved in 0.046 M Tris buffer (200 μL, pH = 8.1) containing 0.01 M CaCl₂, and the hydrolysis was followed by RP-HPLC for 5 days.

The results of these enzymatic hydrolyses are consistent with our findings that analogues containing an LAgl derivative in position 6, 7, 10, or 11 show higher binding affinity and selectivity for sst$_4$ than analogues with a DAgl derivative in the same position in the sequence.

Receptor Autoradiography. CHO-K1 or CLL39 cells stably expressing the cloned five human sst's were grown as described previously.[43,56] All cell culture reagents were supplied by Gibco BRL, Life Technologies (Grand Island, NY). The receptor autoradiographical experiments were performed using ^{125}I-[Leu^8,DTrp^{22},Tyr^{25}]SRIF-28 as extensively described previously.[43]

Adenylate Cyclase Activity. Modulation of forskolin-stimulated adenylate cyclase activity was determined using a radioimmunoassay measuring intracellular cAMP levels by competition binding.[30] sst$_4$-expressing CLL39 cells[30] were subcultured in poly-D-lysine-coated 96-well culture plates at 2×10^4 cells/well and grown for 24 h. Culture medium was removed from the wells, and 100 μL of fresh medium containing 0.5 mM IBMX was added to each well. Cells were incubated for 30 min at 37 °C. Medium was then removed and replaced with fresh medium containing 0.5 mM IBMX, with or without 10 μM forskolin and various concentrations of peptides. Cells were incubated for 30 min at 37 °C. After removal of medium, cells were lysed and cAMP accumulation was determined using a commercially available cAMP scintillation proximity assay (SPA) system according to the instructions from the manufacturer (RPA 538, Amersham Biosciences, Little Chalfont, UK). cAMP data were expressed as percentage of stimulation over the nonstimulated level. Values of EC$_{50}$ (the agonist concentration causing 50% of its maximal effect) were derived from concentration−response curves.

References

(1) Burgus, R.; Dunn, T.; Desiderio, D.; Ward, D.; Vale, W. W.; Guillemin, R. Characterization of the ovine hypothalamic hypophysiotropic TSH-releasing factor (TRF). *Nature* **1970**, *226*, 321−325.

(2) Matsuo, H.; Baba, Y.; Nair, R. M.; Arimura, A.; Schally, A. V. Structure of the porcine LH- and FSH-releasing hormone. I. The proposed amino acid sequence. *Biochem. Biophys. Res. Commun.* **1971**, *43*, 1334−1339.

(3) Burgus, R.; Butcher, M.; Amoss, M.; Ling, N.; Monahan, M.; Rivier, J.; Fellows, R.; Blackwell, R.; Vale, W. W.; Guillemin, R. Primary structure of the ovine hypothalamic luteinizing hormone-releasing factor (LRF). *Proc. Natl. Acad. Sci. U.S.A.* **1972**, *69*, 278−282.

(4) Brazeau, P.; Vale, W. W.; Burgus, R.; Ling, N.; Butcher, M.; Rivier, J. E.; Guillemin, R. Hypothalamic polypeptide that inhibits the secretion of immunoreactive pituitary growth hormone. *Science* **1973**, *179*, 77−79.

(5) Vale, W.; Spiess, J.; Rivier, C.; Rivier, J. Characterization of a 41 residue ovine hypothalamic peptide that stimulates the secretion of corticotropin and β-endorphin. *Science* **1981**, *213*, 1394−1397.

(6) Rivier, J.; Spiess, J.; Thorner, M.; Vale, W. Characterization of a growth hormone releasing factor from a human pancreatic islet tumor. *Nature* **1982**, *300*, 276−278.

(7) Guillemin, R.; Brazeau, P.; Bohlen, P.; Esch, F.; Ling, N.; Wehrenberg, W. B. Growth hormone-releasing factor from a human pancreatic tumor that caused acromegaly. *Science* **1982**, *218*, 585−587.

(8) Koerber, S. C.; Rizo, J.; Struthers, R. S.; Rivier, J. E. Consensus bioactive conformation of cyclic GnRH antagonists defined by NMR and molecular modeling. *J. Med. Chem.* **2000**, *43*, 819−828.

(9) Patel, Y. C.; Wheatley, T. In vivo and in vitro plasma disappearance and metabolism of somatostatin-28 and somatostatin-14 in the rat. *Endocrinology* **1983**, *112*, 220−225.

(10) Bruno, J. F.; Xu, Y.; Song, J.; Berelowitz, M. Molecular cloning and functional expression of a brain-specific somatostatin receptor. *Proc. Natl. Acad. Sci. U.S.A.* **1992**, *89*, 11151−11155.

(11) Yasuda, K.; Rens-Domiano, S.; Breder, C. D.; Law, S. F.; Saper, C. B.; Reisine, T.; Bell, G. I. Cloning of a novel somatostatin receptor, SSTR3, that is coupled to adenylyl cyclase. *J. Biol. Chem.* **1992**, *267*, 20422−20428.

(12) Rohrer, L.; Raulf, F.; Bruns, C.; Buettner, R.; Hofstaedter, F.; Schule, R. Cloning and characterization of a fourth human somatostatin receptor. *Proc. Natl. Acad. Sci. U.S.A.* **1993**, *90*, 4196−4200.

(13) Xu, Y.; Song, H.; Bruno, J. F.; Berelowitz, M. Molecular cloning and sequencing of a human somatostatin receptor, hSSTR4. *Biochem. Biophys. Res. Commun.* **1993**, *193*, 648−652.

(14) Yamada, Y.; Post, S. R.; Wang, K.; Medical, H.; Tager, S.; Bell, G. I.; Seino, S. Cloning and functional characterization of a family of human and mouse somatostatin receptors expressed in brain, gastrointestinal tract, and kidney. *Proc. Natl. Acad. Sci. U.S.A.* **1992**, *89*, 251−255.

(15) Yamada, Y.; Reisine, T.; Law, S. F.; Ihara, Y.; Kubota, A.; Kagimoto, S.; Seino, M.; Seino, Y.; Bell, G. I.; Seino, S. Somatostatin receptors, an expanding gene family: Cloning and functional characterization of human SSTR3, a protein coupled to adenylyl cyclase. *Mol. Endocrinol.* **1992**, *6*, 2136−2142.

(16) Yamada, Y.; Kagimoto, S.; Kubota, A.; Yasuda, K.; Masuda, K.; Someya, Y.; Ihara, Y.; Li, Q.; Imura, H.; Seino, S.; Seino, Y. Cloning, functional expression and pharmacological characterization of a fourth (hSSTR4) and fifth (hSSTR5) human somatostatin receptor subtype. *Biochem. Biophys. Res. Commun.* **1993**, *195*, 844−852.

(17) Patel, Y. C. Somatostatin and its receptor family. *Front. Neuroendocrinol.* **1999**, *20*, 157−198.

(18) Brazeau, P.; Vale, W.; Burgus, R.; Ling, N.; Butcher, M.; Rivier, J.; Guillemin, R. Hypothalamic polypeptide that inhibits the secretion of immunoreactive pituitary growth hormone. *Science* **1973**, *179*, 77−79.

(19) Guillemin, R.; Gerich, J. E. Somatostatin: physiological and clinical significance. *Annu. Rev. Med.* **1976**, *27*, 379−388.

(20) Reichlin, S. Somatostatin. *N. Engl. J. Med.* **1983**, *309*, 1495−1501.

(21) Reichlin, S. Somatostatin (second of two parts). *N. Engl. J. Med.* **1983**, *309*, 1556−1563.

(22) Epelbaum, J. Somatostatin in the central nervous system: physiology and pathological modification. *Prog. Neurobiol.* **1986**, *27*, 63−100.

(23) Sassolas, G. The role of Sandostatin in acromegaly. *Metabolism: Clin., Exp.* **1992**, *41*, 39−43.

(24) Wynick, D.; Bloom, S. R. Clinical review 23: The use of the long-acting somatostatin analog octreotide in the treatment of gut neuroendocrine tumors. *J. Clin. Endocrinol. Metab.* **1991**, *73*, 1−3.

(25) Janecka, A.; Zubrzycka, M.; Janecki, T. Review: Somatostatin analogs. *J. Pept. Res.* **2001**, *58*, 91−107.

(26) Schally, A. V.; Comaru-Schally, A. M.; Nagy, A.; Kovacs, M.; Szepeshazi, K.; Plonowski, A.; Varga, J. L.; Halmos, G. Hypothalamic hormones and cancer. *Front. Neuroendocrinol.* **2001**, *22*, 248−291.

(27) Hannon, J. P.; Nunn, C.; Stolz, B.; Bruns, C.; Weckbecker, G.; Lewis, I.; Troxler, T.; Hurth, K.; Hoyer, D. Drug design at peptide receptors: somatostatin receptor ligands. *J. Mol. Neurosci.* **2002**, *18*, 15−27.

(28) de Herder, W. W.; Lamberts, S. W. Somatostatin and somatostatin analogues: diagnostic and therapeutic uses. *Curr. Opin. Oncol.* **2002**, *14*, 53−57.

(29) Rivier, J. E.; Hoeger, C.; Erchegyi, J.; Gulyas, J.; DeBoard, R.; Craig, A.; Koerber, S. C.; Wenger, S.; Waser, B.; Schaer, J.-C.; Reubi, J. C. Potent somatostatin undecapeptide agonists selective for somatostatin receptor 1 (sst1). *J. Med. Chem.* **2001**, *44*, 2238−2246.

(30) Reubi, J. C.; Schaer, J.-C.; Wenger, S.; Hoeger, C.; Erchegyi, J.; Waser, B.; Rivier, J. SST3-selective potent peptidic somatostatin receptor antagonists. *Proc. Natl. Acad. Sci. U.S.A.* **2000**, *97*, 13973−13978.

(31) Erchegyi, J.; Penke, B.; Simon, L.; Michaelson, S.; Wenger, S.; Waser, B.; Cescato, R.; Schaer, J.-C.; Reubi, J. C.; Rivier, J. Novel sst₄-selective somatostatin (SRIF) agonists. 2. Analogues with β-methyl-3-(2-naphthyl)alanine substitutions at position 8. *J. Med. Chem.* **2003**, *46*, 5587−5596 (in this issue).

(32) Erchegyi, J.; Waser, B.; Schaer, J.-C.; Cescato, R.; Rivier, J.; Reubi, J. C. Novel sst₄-selective somatostatin (SRIF) agonists. 3. Analogues amenable to radiolabeling. *J. Med. Chem.* **2003**, *46*, 5597−5605 (in this issue).

(33) Grace, C. R. R.; Erchegyi, J.; Koerber, S. C.; Reubi, J. C.; Rivier, J.; Riek, R. Novel sst₄-selective somatostatin (SRIF) agonists. 4. Three-dimensional consensus structure by NMR. **2003**, *46*, 5606−5618 (in this issue).

(34) Qasmi, D.; René, L.; Badet, B. An α-aminoglycine derivative suitable for solid phase peptide synthesis using Fmoc strategy. *Tetrahedron Lett.* **1993**, *34*, 3861−3862.

(35) Sypniewski, M.; Penke, B.; Simon, L.; Rivier, J. (R)-tert-Butoxycarbonylamino-fluorenylmethoxycarbonyl-glycine from (S)-Benzyloxycarbonyl-serine or from papain resolution of the corresponding amide or methyl ester. *J. Org. Chem.* **2000**, *65*, 6595−6600.

(36) Jiang, G.-C.; Simon, L.; Rivier, J. E. Orthogonally protected N-methyl-substituted α-aminoglycines. *Protein Pept. Lett.* **1996**, *3*, 219−224.

(37) Jiang, G.; Miller, C.; Koerber, S. C.; Porter, J.; Craig, A. G.; Bhattacharjee, S.; Kraft, P.; Burris, T. P.; Campen, C. A.; Rivier, C. L.; Rivier, J. E. Betidamino acid scan of the GnRH antagonist Acyline. *J. Med. Chem.* **1997**, *40*, 3739−3748.

(38) Cervini, L.; Theobald, P.; Corrigan, A.; Craig, A. G.; Rivier, C.; Vale, W.; Rivier, J. Corticotropin releasing factor (CRF) agonists with reduced amide bonds and Ser⁷ substitutions. *J. Med. Chem.* **1999**, *42*, 761−768.

(39) Rivier, J. E.; Jiang, G.-C.; Koerber, S. C.; Porter, J.; Craig, A. G.; Hoeger, C. Betidamino acids: Versatile and constrained scaffolds for drug discovery. *Proc. Natl. Acad. Sci. U.S.A.* **1996**, *93*, 2031−2036.

(40) Vale, W.; Rivier, C.; Brown, M.; Rivier, J. Pharmacology of TRF, LRF and somatostatin. *Hypothalamic Peptide Hormones and Pituitary Regulation: Advances in Experimental Medicine and Biology*; Plenum Press: New York, 1977; pp 123−156.

(41) Vale, W.; Rivier, J.; Ling, N.; Brown, M. Biologic and immunologic activities and applications of somatostatin analogs. *Metabolism* **1978**, *27*, 1391−1401.

(42) Kaljuste, K.; Undén, A. New method for the synthesis of N-methyl amino acids containing peptides by reductive methylation of amino groups on the solid phase. *Int. J. Pept. Protein Res.* **1993**, *42*, 118−124.

(43) Reubi, J. C.; Schaer, J. C.; Waser, B.; Wenger, S.; Heppeler, A.; Schmitt, J. S.; Mäcke, H. R. Affinity profiles for human somatostatin receptor sst1-sst5 of somatostatin radiotracers selected for scintigraphic and radiotherapeutic use. *Eur. J. Nucl. Med.* **2000**, *27*, 273−282.

(44) Reubi, J. C.; Schaer, J. C.; Waser, B.; Hoeger, C.; Rivier, J. A selective analog for the somatostatin sst₁-receptor subtype expressed by human tumors. *Eur. J. Pharmacol.* **1998**, *345*, 103−110.

(45) Rohrer, S. P.; Birzin, E. T.; Mosley, R. T.; Berk, S. C.; Hutchins, S. M.; Shen, D.-M.; Xiong, Y.; Hayes, E. C.; Parmar, R. M.; Foor, F.; Mitra, S. W.; Degrado, S. J.; Shu, M.; Klopp, J. M.; Cai, S.-J.; Blake, A.; Chan, W. W. S.; Pasternak, A.; Yang, L.; Patchett, A. A.; Smith, R. G.; Chapman, K. T.; Schaeffer, J. M. Rapid identification of subtype-selective agonists of the somatostatin receptor through combinatorial chemistry. *Science* **1998**, *282*, 737−740.

(46) Bass, R. T.; Buckwalter, B. L.; Patel, B. P.; Pausch, M. H. P. L. A.; Strnad, J.; Hadcock, J. R. Identification and characterization of novel somatostatin antagonists. *Mol. Pharmacol.* **1996**, *50*, 709−715.

(47) Bass, R. T.; Buckwalter, B. L.; Patel, B. P.; Pausch, M. H. P. L. A.; Strnad, J.; Hadcock, J. R. Identification and characterization of novel somatostatin antagonists. *Mol. Pharmacol.* **1997**, *51*, 170 Erratum.

(48) Hocart, S. J.; Jain, R.; Murphy, W. A.; Taylor, J. E.; Morgan, B.; Coy, D. H. Potent antagonists of somatostatin: Synthesis and biology. *J. Med. Chem.* **1998**, *41*, 1146−1154.

(49) Hocart, S. J.; Jain, R.; Murphy, W. A.; Taylor, J. E.; Coy, D. H. Highly potent cyclic disulfide antagonists of somatostatin. *J. Med. Chem.* **1999**, *42*, 1863−1871.

(50) Rajeswaran, W. G.; Hocart, S. J.; Murphy, W. A.; Taylor, J. E.; Coy, D. H. Highly potent and subtype selective ligands derived by N-methyl scan of a somatostatin antagonist. *J. Med. Chem.* **2001**, *44*, 1305−1311.

(51) Nutt, R. F.; Veber, D. F.; Curley, P. E.; Saperstein, R.; Hirschmann, R. Somatostatin analogs which define the role of the lysine-9 amino group. *Int. J. Pept. Protein Res.* **1983**, *21*, 66–73.

(52) Stewart, J. M.; Young, J. D. Solid-Phase Peptide Synthesis. *Solid-Phase Peptide Synthesis*, 2nd ed.; Pierce Chemical Co.: Rockford, IL, 1984; p 176.

(53) Miller, C.; Rivier, J. Peptide chemistry: Development of high-performance liquid chromatography and capillary zone electrophoresis. *Biopolymers* **1996**, *40*, 265–317.

(54) Miller, C.; Rivier, J. Analysis of synthetic peptides by capillary zone electrophoresis in organic/aqueous buffers. *J. Pept. Res.* **1998**, *51*, 444–451.

(55) Hoeger, C. A.; Galyean, R. F.; Boublik, J.; McClintock, R. A.; Rivier, J. E. Preparative reversed phase high performance liquid chromatography. II. Effects of buffer pH on the purification of synthetic peptides. *Biochromatography* **1987**, *2*, 134–142.

(56) Schulz, S.; Pauli, S. U.; Handel, M.; Dietzmann, K.; Firsching, R.; Hollt, V. Immunohistochemical determination of five somatostatin receptors in meningioma reveals frequent overexpression of somatostatin receptor subtype sst2A. *Clin. Cancer Res.* **2000**, *6*, 1865–1874.